A Multiple Degree-of-Freedom Approach to Nonlinear Beam Vibrations

JAMES A. BENNETT*
University of Illinois, Urbana, Ill.
AND
JOE G. EISLEY†
University of Michigan, Ann Arbor, Mich.

The steady-state free and forced response and stability for large amplitude motion of a beam with clamped ends is investigated. Elastic restraint of the ends is included in order to relate theory with experiment. A multimode analytical and numerical technique is used to obtain theoretical solutions for both response and stability. Experimental results largely confirm the results of the analysis. It is concluded that, while single mode analyses are adequate in some cases, there are circumstances where a multimode analysis is essential to predict the observed results.

Nomenclature

A_m	= amplitude of the mth mode
E	= Young's modulus
F	= transverse force
F_0	= generalized force
h	= beam thickness
I	= second moment of area of the cross section
K_s	= axial spring factor
k	= axial spring constant
k_1	= rotational spring constant
L	= beam length
P_0	= initial axial tension
P_{0m}	= nondimensional amplitude of the generalized harmonic force
t	= time
w	= transverse displacement
x	= axial coordinate
$M_{mkin},F_{1m},G_{mrs},G_{mqrs}$	= modal constants
η	= nondimensional axial coordinate
λ	= ratio of axial load to fundamental Euler buckling load
ξ_m	= generalized coordinate
ρ	= mass density
$\tau,\bar{t}$	= nondimensional time
Φ_m,Φ	= assumed spatial function or linear mode shape
ϕ_m	= nondimensional linear mode shape
ψ_n	= eigenvalue of the linear free problem
ω	= nondimensional frequency
ω_0	= linear natural frequency

1. Introduction

THE nonlinear transverse vibrations of a beam whose ends are restrained from axial displacement has received much attention. The common approach is to assume some form for the spatial solution, usually a linear mode shape, and then solve the nonlinear ordinary differential equation that results for the time variable. Most of this work has been concerned with simply supported end conditions only. The majority of authors have used only a single assumed spatial function to accomplish this; however, McDonald[1] has solved the free vibration problem for an arbitrary initial condition using an expansion of elliptic functions which are the exact solutions to the free single mode problem. Srinivasan[2] has applied a general modal approach in discussing a simply supported beam and has obtained response solutions including several modes.

The stability of the steady-state solution of forced motion has received much less attention, although Eisley[3] pointed out that there were regions in which the single mode solution was not stable. The problem of the parametric excitation of a mode which is initially at rest has been discussed by the authors.[4]

There has been very little experimental verification of the theoretical results which have been obtained for this problem. Some early work was done by Burgreen.[5] Experimental work on the nonlinear response of beams to random inputs has been reviewed by Lyon.[6]

In the investigation reported here the response and stability of multiple mode, large amplitude, transverse vibrations of a beam were predicted by approximate analytical and numerical techniques and the results were then compared to experimentally determined values. General equations for the response and stability of a multiple degree-of-freedom beam were derived and results then obtained for the particular case which describes the experiment. The experimental beam was, ideally, clamped on both ends; however, because not all the elasticity of the support could be removed, a term to express the axial elasticity of the support and another term to express elastic rotational end restraint were included in the analysis.

2. Equations of Motion

The partial differential equation describing the transverse vibration of a beam which is axially restrained and in which large deflections are permitted is[7]

$$\rho h \frac{\partial^2 w}{\partial t^2} + EI \frac{\partial^4 w}{\partial x^4} - \left[P_0 + K_s \frac{hE}{2L} \int_0^L \left(\frac{\partial w}{\partial x} \right)^2 dx \right] \frac{\partial^2 w}{\partial x^2} = F(x,t) \quad (1)$$

where K_s is a factor expressing the amount of end restraint

$$K_s = L/hE(1/k + L/hE)^{-1}$$

Thus $K_s = 1.0$ is fully restrained, and $K_s = 0.0$ represents no end restraint.

The only nonlinear effect that has been included is that due to the effect of the transverse deflection on the axial force

Received April 14, 1969, revision received November 3, 1969
This work was substantially supported by NSF Grant GR-1251 and this support is gratefully acknowledged. This work forms part of a thesis submitted in partial fulfillment of the Ph.D. requirement at the University of Michigan by J. A. Bennett.

* Assistant Professor, Department of Aeronautical and Astronautical Engineering. Associate AIAA.
† Professor, Department of Aerospace Engineering. Associate Fellow AIAA.

developed due to end restraint. The curvatures are still restricted to be small and both shear deformations and longitudinal inertia have been neglected.

Assume that

$$w(x,t) = \sum_{i=1}^{j} \xi_i(t)\Phi_i(x) \tag{2}$$

and specify that $\Phi_i(x)$ satisfies the associated linear problem

$$\rho h \frac{\partial^2 w}{\partial t^2} + EI \frac{\partial^4 w}{\partial x^4} - P_0 \frac{\partial^2 w}{\partial x^2} = 0$$

and the appropriate boundary conditions. It is therefore practical to include any elastic rotational end restraint in the linear problem. Then, applying Galerkin's method, the following set of nonlinear ordinary differential equations are obtained:

$$\frac{d^2\xi_m}{d\tau^2} + F_{1m}\xi_m + \sum_{k=1}^{j}\sum_{i=1}^{j}\sum_{n=1}^{j} K_s M_{mkin}\xi_k\xi_i\xi_n = F_{0m}(\tau) \tag{3}$$

$$m = 1,2, \ldots j$$

$$F_{1m} = (IL^2/h)\Psi_m{}^4$$

$$M_{mkin} = -\frac{1}{2}\frac{\int_0^1 \frac{d\phi_k}{d\eta}\frac{d\phi_i}{d\eta}d\eta \int_0^1 \frac{d^2\phi_n}{d\eta^2}\phi_m d\eta}{\int_0^1 \phi_m{}^2 d\eta}$$

$$F_{0m} = \frac{L}{Eh}\frac{\int_0^1 F(\eta,\tau)\phi_m d\eta}{\int_0^1 \phi_m{}^2 d\eta}$$

where the following nondimensional quantities have been defined:

$$\tau = (E/\rho)^{1/2}t/L, \quad \eta = x/L, \quad \phi_m = \Phi_m/L$$

3. Response

Since there is no known exact solution to Eq. (3), it will be necessary to turn to an approximate solution. The method of harmonic balance will be used. The method involves assuming a solution of summed harmonics, substituting this assumed solution into the differential equations, and then equating the coefficients of the harmonics to zero. Any harmonics which arise in the substitution which are not included in the assumed solution are neglected. The effectiveness of this method is dependent on choosing only those harmonics which will be important. It has been found, for the Duffing equation obtained for a single assumed mode, that a single harmonic term in the time expansion gives accurate results over a wide range of interest. It is also known that when damping is neglected, only in phase and out of phase motions arise.

Thus, for harmonic forcing, assume a solution of the form

$$\xi_m(\tau) = A_m \cos\omega\tau \tag{4}$$

Substituting Eq. (4) into Eq. (3) and neglecting the terms that contain $\cos 3\omega\tau$, the following is obtained:

$$-A_m\omega^2 + F_{1m}A_m + \tfrac{3}{4}K_s\sum_{k=1}^{j}\sum_{i=1}^{j}\sum_{n=1}^{j} M_{mkin}A_kA_iA_n = P_{0m} \tag{5}$$

This set of j nonlinear algebraic equations relating the jA_m's and ω may be solved on a digital computer by the Wegstein iteration technique.[8] The solutions were started for a given initial ω using the appropriate single mode equation. The solutions were then continued by incrementing ω and using the solutions for the previous ω as initial guesses. Since only real values of the A_m's were important, no attempt was made to find complex values of the A_m's.

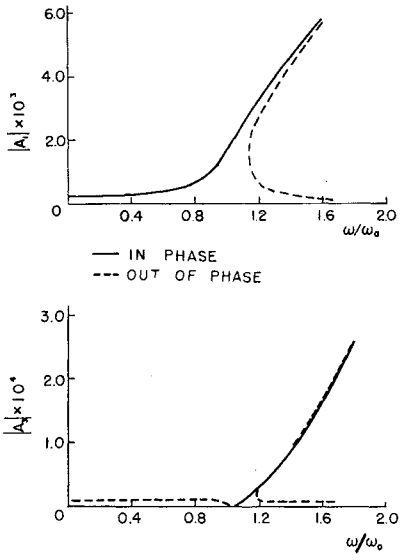

Fig. 1 Symmetric forcing, first and third modes, $0 \leq \omega/\omega_0 \leq 2.0$, $\lambda = 0.0$.

4. Response for a Particular Example

For the case under consideration, the equations for the first three modes can be expressed in the following form. The coefficients may be evaluated by numerical integration and the fact that several of the coefficients are zero has been used to simplify the equations.

$$d^2\xi_1/d\tau^2 + F_{11}\xi_1 + K_s[G_{111}\xi_1{}^3 + G_{121}\xi_2{}^2\xi_1 + G_{131}\xi_3{}^2\xi_1 + G_{113}\xi_1{}^2\xi_3 + G_{333}\xi_3{}^3] = P_{01}\cos\omega\tau \tag{6}$$

$$d^2\xi_2/d\tau^2 + F_{12}\xi_2 + K_s[G_{212}\xi_1{}^2\xi_2 + G_{232}\xi_3{}^2\xi_2 + G_{222}\xi_2{}^3 + G_{2123}\xi_1\xi_2\xi_3] = P_{02}\cos\omega\tau$$

$$d^2\xi_3/d\tau^2 + F_{13}\xi_3 + K_s[G_{311}\xi_1{}^3 + G_{321}\xi_2{}^2\xi_1 + G_{331}\xi_3{}^2\xi_1 + G_{313}\xi_1{}^2\xi_3 + G_{333}\xi_3{}^3] = P_{03}\cos\omega\tau$$

$$G_{mrs} = M_{mrrs} + M_{mrsr} + M_{msrr}$$

$$G_{mqrs} = M_{mqrs} + M_{mqsr} + M_{msqr} + M_{msrq} + M_{mrsq} + M_{mrqs}$$

In general, two types of problems arise: 1) symmetric forcing, and 2) asymmetric forcing.

A. Symmetric Forcing

If the force is applied at $L/2$ or if it is symmetric about $L/2$, P_{02} is identically zero as are all the P_{0m}'s for the even numbered modes.

The response for the single mode has been discussed extensively in the literature and is the typical response for the hard spring oscillator. Since the generalized forces for the even numbered modes are zero, the solution will indicate that these modes will not respond. The response for the first and third modes is shown in Fig. 1 for $0 \leq \omega/\omega_0 \leq 2.0$, and in Fig. 2 for $5.4 \leq \omega/\omega_0 \leq 7.0$, where ω_0 is the linear natural frequency of the first mode. The expected fundamental resonances of A_1 in the neighborhood of the first linear natural frequency occur. However, there is also an A_3 resonance in the neighborhood of the first linear natural frequency and an A_1 resonance in the neighborhood of the third linear natural frequency. This type of resonance due to nonlinear coupling will be called "coupling resonance." At $\omega/\omega_0 = 1.3$ the coupling resonance causes approximately a 2% distortion in the spatial response as shown in Fig. 3. The effect in the first linear natural frequency region is to flatten the response shape as the frequency increases. The

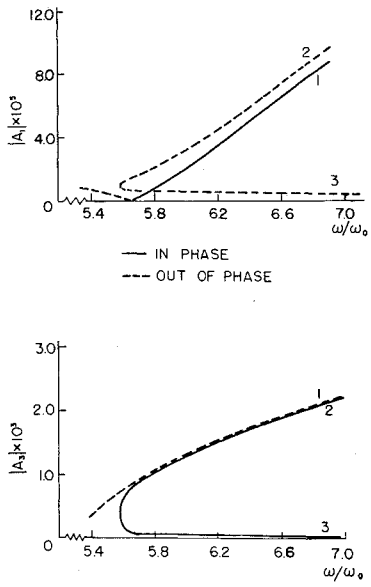

Fig. 2. Symmetric forcing, first and third modes, $5.4 \leq \omega/\omega_0 \leq 7.0$, $\lambda = 0.0$.

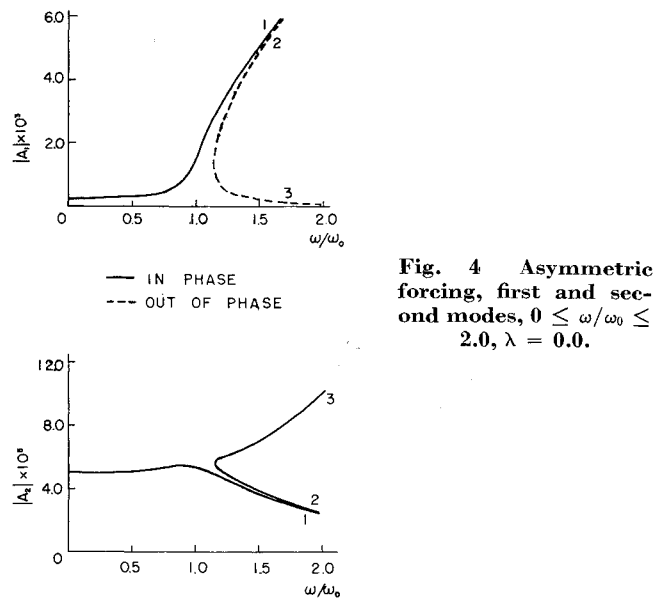

Fig. 4 Asymmetric forcing, first and second modes, $0 \leq \omega/\omega_0 \leq 2.0$, $\lambda = 0.0$.

ratio of A_3/A_1 increases with increasing ω/ω_0 in the region of the first mode resonance, thus, the contribution of A_3 to the response shape increases for increasing ω/ω_0 in this region.

B. Asymmetric Forcing

When the beam is forced asymmetrically, the second mode enters into the response. This response will be generated by forcing the beam at $L/4$.

The response for modes 1 and 2 is shown in Fig. 4. Of particular interest is the absence of a coupling resonance. Although there are three separate branches of the curve in this area, there is no significant increase in amplitude of either mode in the resonance region of the other mode. This can be explained by examining the coupling terms of the three modes. In the equations for modes 1 and 3, there is a term of the type ξ_3^3 in the former and ξ_1^3 in the latter. If, say, ξ_1 becomes large, the term in the third mode equation will also become relatively large and will significantly influence the ξ_3 response. However, the coefficients of the ξ_1^3 and ξ_3^3 terms in the second mode equation are zero; thus, there is no significant coupling between the resonant odd modes. In fact, the coupling between the first and second, and the third and second modes is so weak that for all practical purposes the nonlinear coupling terms may be dropped and the second-mode response calculated from

$$\omega^2 = F_{12} + \tfrac{3}{4}K_s G_{222} A_2^2 - P_{02}/A_2 \qquad (7)$$

Comparing this response with the complete three mode response, differences of less than 1% were noted. If this simplification is made, the multiple solutions for ξ_2 corresponding to the multiple solutions for ξ_1 and ξ_3 do not occur.

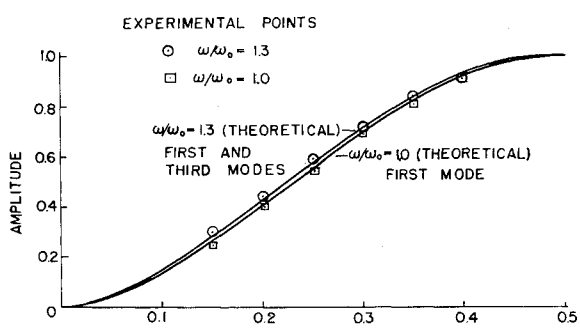

Fig. 3 Response shapes, first mode resonance, $\lambda = 0.0$

If higher-order modes were included, this pattern of coupling would continue except that the even modes would also be coupled through the cubic term. It is interesting to note that the type of coupling and thus the type and number of coupling resonances are dependent on the boundary conditions. Reference to Eq. (3) indicates that the coefficient of this term in the mth equation for kth mode coupling is governed by an integral of the form

$$\int_0^1 \frac{d^2\phi_n}{d\eta^2}\,\phi_m d\eta$$

If the beam is simply supported at both ends, this term is identically zero for all choices of $m \neq k$, since the linear mode shapes are $\phi_n = \sin(n\pi\eta)$. Thus, there will be no coupling resonances in a beam which is simply supported at both ends. On the other hand, if one end is clamped and one is simply supported, the evaluation of this integral indicates that all modes are coupled through the cubic term.

A common approximation to the clamped-clamped beam is

$$\phi_n = \tfrac{1}{2}[1 - \cos(2n\pi\eta)]$$

Evaluation of the integral in Eq. (3) for this mode shape indicates that none of the modes are coupled through the cubic term. This indicates that one must be extremely careful in the choice of mode shapes and the number of modes that are retained.

5. Stability

Although a solution has been found to the steady-state problem there is neither assurance that these solutions are unique nor that they are stable solutions because of the nonlinearity of the equations. Thus, it will be necessary to check the stability of these solutions and to investigate the possibility of further steady-state solutions.

The stability question will be investigated by studying the behavior of a small perturbation of the steady-state response. Let $\xi_m = \xi_{ms} + \delta\xi_m$ where ξ_{ms} is the steady state solution for Eq. (3), and $\delta\xi_m$ is a small perturbation of the mth mode. Substituting this into Eq. (3), and retaining only first-order terms, the following is obtained.

$$\frac{d^2\delta\xi_m}{d\tau^2} + F_{1m}\delta\xi_m + K_s \sum_{k=1}^{j}\sum_{i=1}^{j}\sum_{n=1}^{j} M_{mkin}(\xi_{is}\xi_{ns}\delta\xi_k + \xi_{ks}\xi_{ns}\delta\xi_i + \xi_{ks}\xi_{is}\delta\xi_n) = 0 \qquad (8)$$

For the stability problem only the symmetric case will be discussed. In the case of a single assumed mode this equa-

tion reduces to a Mathieu type equation whose stability is well known. If just two modes are included the following pair of Mathieu equations occur:

$$\frac{d^2\delta\xi_1}{d\bar{t}^2} + \frac{1}{4\omega^2}\left[F_{11} + \frac{3K_sG_{111}A_1^2}{2} + \frac{3G_{111}K_sA_1^2}{2}\cos\bar{t}\right]\delta\xi_1 = 0 \tag{9}$$

$$\frac{d^2\delta\xi_2}{d\bar{t}^2} + \frac{1}{4\omega^2}\left[F_{12} + \frac{K_sG_{212}A_1^2}{2} + \frac{K_sG_{212}A_1^2}{2}\cos\bar{t}\right]\delta\xi_2 = 0$$

where $\bar{t} = 2\omega\tau$. These two Mathieu type equations are uncoupled and the first one is identical to the case for one mode.

It is known that the solutions to the Mathieu equation in the regions of instability are of the form $e^{\mu\bar{t}}[\beta(\bar{t})]$. If $\beta(\bar{t})$ is expanded in powers of a small parameter, the leading term is periodic with period $4\pi/n$, where n is the integer number of the stability region. This is discussed in detail by Hayashi.[9] Thus, the instabilities that arise must be of the form

$$\delta\xi_m = A_m \cos n\omega\tau$$

For $n > 1$ this response is called ultraharmonic. Thus, the first instability region in the Mathieu diagram maps into the jump instability region in the A, ω plane. The subsequent regions are identified with the integer order ultraharmonics. If there is some damping in the system, only the lower order ultraharmonics can be expected to arise. Two distinct types of instability arise:

1) first mode instability,
$\delta\xi_1 = A_1 \cos n\omega\tau$, $\delta\xi_2 = 0$, $n = 1,2,3 \ldots$
2) second mode instability,
$\delta\xi_1 = 0$, $\delta\xi_2 = A_2 \cos n\omega\tau$, $n = 1,2,3 \ldots$

The appearance of a second mode is of particular interest because it is normally at rest. If only the linear terms are considered, the rest mode must stay at rest; but, due to the nonlinear coupling, the rest mode may be excited. This type of behavior has been discussed by the authors in a previous paper[4] in some detail. The stability regions for modes 1 and 2 only are presented in Fig. 5.

For the case when all three modes are considered, the perturbation equations will take the form

$$\frac{d^2\delta\xi_1}{d\bar{t}^2} + \frac{1}{4\omega^2}\left[F_{11} + K_s\left(\frac{3G_{111}A_1^2}{2} + \frac{G_{131}A_3^2}{2} + G_{113}A_1A_3\right)(1.0 + \cos\bar{t})\right]\delta\xi_1 + \frac{1}{4\omega^2}\left[K_s\left(G_{131}A_1A_3 + \frac{G_{113}A_1^2}{2} + \frac{3G_{133}A_3^2}{2}\right)(1.0 + \cos\bar{t})\right]\delta\xi_3 = 0 \tag{10}$$

$$\frac{d^2\delta\xi_2}{d\bar{t}^2} + \frac{1}{4\omega^2}\left[F_{12} + K_s\left(\frac{G_{212}A_1^2}{2} + \frac{G_{232}A_3^2}{2} + \frac{G_{1123}}{2}A_1A_3\right) \times (1.0 + \cos\bar{t})\right]\delta\xi_2 = 0$$

$$\frac{d^2\delta\xi_3}{d\bar{t}^2} + \frac{1}{4\omega^2}\left[F_{13} + K_s\left(\frac{3G_{333}A_3^2}{2} + \frac{G_{313}A_1^2}{2} + G_{331}A_1A_3\right) \times (1.0 + \cos\bar{t})\right]\delta\xi_3 + \frac{1}{4\omega^2}\left[K_s\left(G_{313}A_1A_3 + \frac{G_{331}A_3^2}{2} + \frac{3G_{311}A_1^2}{2}\right)(1.0 + \cos\bar{t})\right]\delta\xi_1 = 0$$

Note that the second equation is independent of the first and third. It is of the Mathieu type and may be solved in a manner analogous to that used before. When the third mode is included, the intercept of the second instability region of the second mode with the response curve shifts about $3\frac{1}{2}\%$ lower in ω/ω_0. The effect on the third and higher regions is infinitesimal.

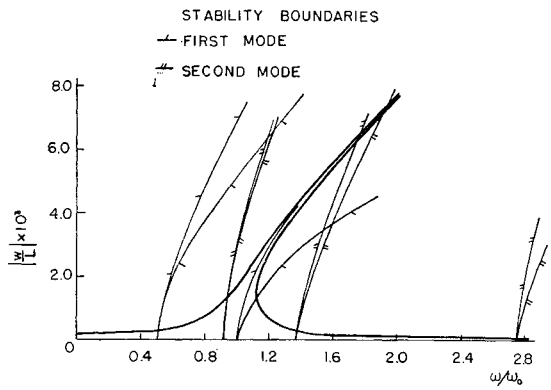

Fig. 5 Symmetric forcing, instability regions for first and second modes, λ = 0.0. Flags are on the stable side of boundary.

The coupled Mathieu type equations of the first and third modes may be analyzed by a direct numerical application of Floquet theory.[10] This involves integrating the equivalent first order differential equations over a period to assemble a matrix, called the monodromy matrix, and then obtaining its eigenvalues. The eigenvalues directly determine the stability of the point under consideration. The method only analyzes one point on the response curve at a time so it is necessary to determine the instability points of several response curves in order to construct regions of instability. Stability boundaries for specific cases are given later in the report and are discussed along with the experimental results

6. Experimental Equipment

An experiment was designed to provide data to augment the theoretical results and to provide insight into the accuracy of the theoretical predictions. The primary information desired was a response curve including regions of instability for a beam. The experimental equipment is discussed more fully in Ref. 7.

The beam was constructed of tool steel, 10 in. × 1 in. × 0.0313 in. It was clamped in steel blocks 6 in. × 6 in. × $4\frac{1}{2}$ in. The clamping surface was 2 in. × 1 in. The beam was located by three steel $\frac{1}{8}$ in. diameter pins. The corresponding holes in the beam were individually reamed to fit the pins. The jaw was held with three $\frac{3}{8}$ n. diameter steel bolts. The mounting blocks were placed in the ways of a lathe bed and held in position by a clamping plate underneath the ways. One end remained attached, but the other end

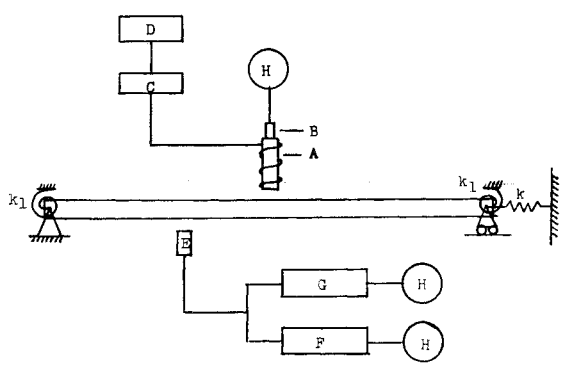

Fig. 6 Experimental schematic: A—horsehoe magnet, B—accelerometer, C—power amplifier, D—function generator, E—displacement sensor, F—filter, G—frequency counter, H—oscilloscope.

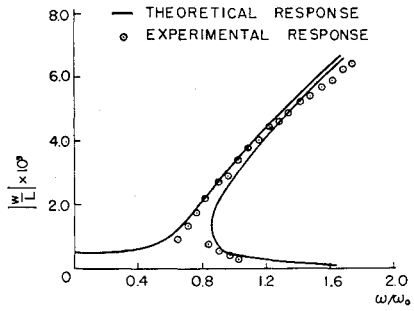

Fig. 7 Symmetric forcing, displacement at $L/2$, $\lambda = 0.5$.

may be loosened to set the initial tension. Two 1 in. × 3 in. steel bars were bolted to the top surfaces of the blocks to increase the bending rigidity of the setup. Despite all attempts to restrain the ends of the beam from moving toward each other, it was discovered that the elasticity of the test rig was a significant factor. This suggested that improperly evaluated boundary conditions may be a prime source of error in previous experiments of this type. The position of the movable block was regulated by a screw arrangement and then the block was clamped into position. The initial axial load on the beam was measured by two foil-type strain gages placed on opposite sides of the beam 1.5 in. from the end.

The beam was forced by an electromagnet as shown in the schematic diagram of Fig. 6. The magnet was designed such that the motion of the beam would not significantly effect the force applied to the beam. The magnet was suspended on thin wires so that the sinusoidal force applied to the beam could be measured directly by placing an accelerometer on the magnet. The magnitude of the sinusoidal force could be kept constant by continuously monitoring the accelerometer output.

The magnet actually applied a forcing function of the type

$$F(\tau) \propto (1 + \cos\omega\tau)$$

If a single mode response is sought and a solution is assumed in the form $\xi_1 = d_1 + A_1 \cos\omega\tau$ where d_1 is a constant, after balancing the harmonics the following equations result:

$$\begin{aligned} -\omega^2 A_1 + F_{11}A_1 + G_{111}K_s(3d_1^2A_1 + \tfrac{3}{4}A_1^3) - P_{01} &= 0 \\ F_{11}d_1 + K_sG_{111}(d_1^3 + \tfrac{3}{2}A_1^2d_1) - P_{01} &= 0 \end{aligned} \tag{11}$$

Near the first-mode resonance region A_1 becomes large and it is possible to neglect d_1^2 compared to A_1^2. Or

$$\begin{aligned} -\omega^2 A_1 + F_{11}A_1 + \tfrac{3}{4}G_{111}K_sA_1^3 - P_{01} &= 0 \\ F_{11}d_1 + K_sG_{111}(\tfrac{3}{2}A_1^2d_1) - P_{01} &= 0 \end{aligned} \tag{12}$$

This essentially uncouples the equations in the resonance region, and also indicates that the sinusoidal amplitude is identical to the case for pure sinusoidal forcing. Outside of the resonance region the response is determined by the linear rather than the nonlinear term.

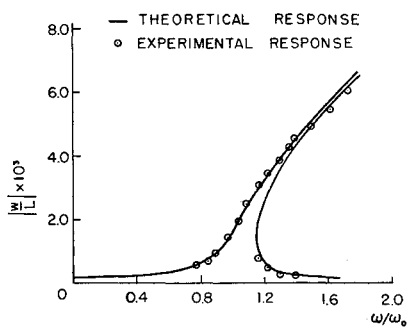

Fig. 8 Symmetric forcing, displacement at $L/2$, $\lambda = 0.0$.

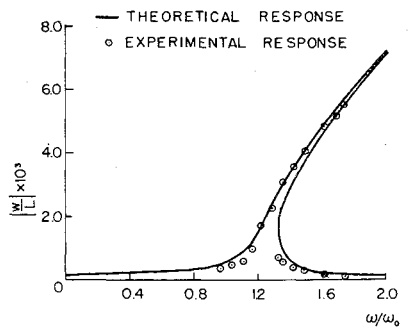

Fig. 9 Symmetric forcing, displacement at $L/2$, $\lambda = -0.5$.

Therefore the sinusoidal part of the response should accurately indicate the response to pure sinusoidal forcing. Equations (11) were solved numerically and indicated that this approximation was accurate to within 1%.

The displacement was measured by a Bently-Nevada eddy current proximeter. The output was linearly related to displacement over the range of displacements that were tested. The instabilities of the first mode were easily detected by the displacement measuring equipment. The instabilities of the higher modes were not always well defined in the displacement trace. Often it was possible to see a disturbance, but its frequency and shape were obscure. To handle this, the output was filtered by a band pass filter. The pass band could be set in the neighborhood of the natural frequency of the mode whose stability was under question. The filtered response would contain primarily the components at this frequency. The order of the harmonic could be easily determined by comparing the filtered and unfiltered response. Thus, the particular mode that was unstable could be determined precisely by moving the displacement proximeter along the beam and observing the phase changes of the filtered response.

The axial spring constant k was determined by measuring the axial strain in the beam with strain gages and comparing the actual stretching of the beam with the stretching which would have been developed if the ends were completely restrained. For the case at hand a value of $K_s = 0.9$ was obtained. The rotational spring constant k_1 was determined by comparing the experimental static deflection curve with the analytical solution for elastic rotational restraints.

7. Experimental Results

Three different values of λ, the initial tension ratio, were used: $\lambda = 0.0$, $\lambda = -0.5$, $\lambda = +0.5$. The theoretical and experimental responses for $\lambda = 0.5, 0.0, -0.5$ are plotted in Figs. 7, 8, and 9, respectively. The experimental forcing corresponded to a value of $P_{01} = 5.0 \times 10^{-8}$ and this value

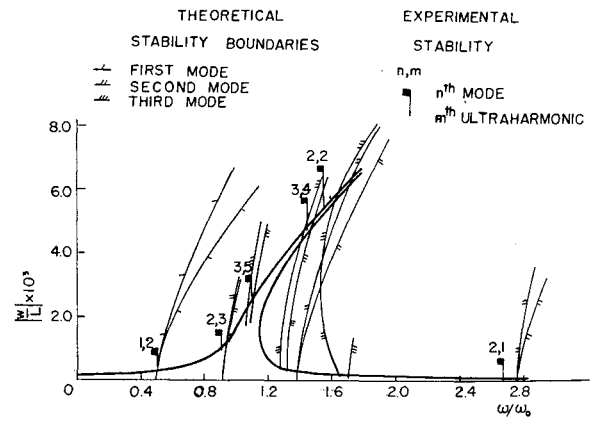

Fig. 10 Theoretical and experimental instabilities, symmetric forcing, $\lambda = 0.0$. Flags are on the stable side of boundary.

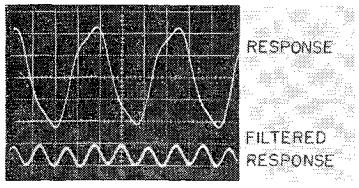

Fig. 11 Third-order ultraharmonic of the second mode, $\lambda = 0.0$.

was used in the theoretical calculation. The theoretical and experimental stability boundaries for $\lambda = 0.0$ are presented in Fig. 10. The results of $\lambda = 0.0$ will be discussed primarily since the results for all values of λ were similar.

A. Lambda = 0.0

The experimental points agree with the theoretical curves quite well with some discrepancy at the higher amplitudes. This will be discussed in terms of the instabilities.

First mode instabilities were observed experimentally in two areas. The jump phenomenon was observed both for increasing and decreasing ω/ω_0. For increasing ω/ω_0, the theory which excludes damping does not predict an instability point, so there can be no confirmation of this. The point of instability for decreasing ω/ω_0 is the point of vertical tangency. This point is confirmed by the experimental results. The first mode was also unstable as a second-order ultraharmonic.

The second mode showed ultraharmonics of the second and third order. The third-order ultraharmonic occurred in an extreme y narrow range of ω/ω_0. An example .s shown in Fig. 11. The second-order ultraharmonic occurred at a lower frequency than was theoretically predicted. This discrepancy was noted for all values of λ. The instability was of significant magnitude and was visible in the response trace. It produced a mode shape that was not symmetric, as Fig. 12 shows. Since energy must be going into the oscillation of the second mode, it must be taken from the first or third mode. Thus, a decrease in first mode amplitude from that predicted from the steady-state theory would be expected. This effect was observed experimentally as was noted earlier, since the experimental points fall below the theoretical curve in the region where the second linear mode is unstable. This instability persisted until the jump occurred, indicating that to precisely determine the jump phenomenon, it would be necessary to include the second mode instabilities in the analysis.

The third mode showed fourth- and fifth-order ultraharmonic instability. The magnitude of the instabilities were not as great as the second mode second order ultraharmonic, but the fourth order third mode ultraharmonic was noticeable in the response over a range of about one cps (Fig. 13). The lower-order ultraharmonics of the third mode occurred after the jump and were not detectable although theoretically the instability regions exist.

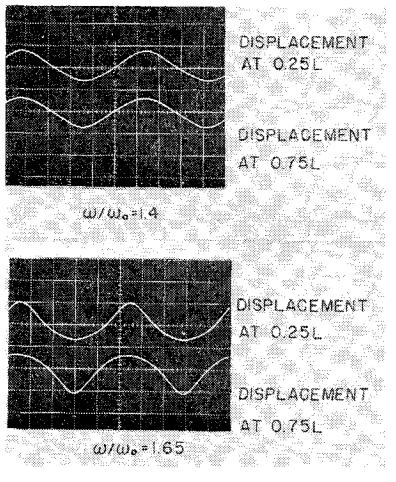

Fig. 12 Second-order ultraharmonic of the second mode, $\lambda = 0.0$.

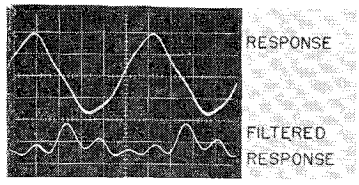

Fig. 13 Fourth-order ultraharmonic of the third mode, $\lambda = 0.0$.

B. Lambda = +0.5

The effect of positive λ is to decrease the linear natural frequency and to increase the hardening effect. The same instabilities discussed in the $\lambda = 0.0$ section were observed for $\lambda = +0.5$.

C. Lambda = −0.5

The effect of negative λ is to increase the linear natural frequency and to decrease the nonlinear hardening. The decrease in the nonlinear effect also decreased the amplitudes of the fifth order ultraharmonic of the third mode and the third-order ultraharmonic of the second mode to the point that they were not observed.

8. Conclusions

The results of the experimental and theoretical studies indicate that the single-term harmonic balance technique gives excellent approximate solutions for the amplitudes encountered in the beam problem (twice the beam thickness). However, the single spatial mode approach must be used with some caution. In problems in which the nonlinear coupling is weak, it is possible to obtain quite accurate response curves by dropping the nonlinear coupling terms and considering each mode individually for response purposes. However, in those cases where the coefficient of the cubic coupling term is nonzero, coupling resonance will appear which may significantly modify the response shapes.

It is also necessary to consider the possibility of modal instabilities. A mode may respond in an ultraharmonic type of response at some multiple of the forcing frequency. It is further necessary to consider the stability of the rest modes because they may oscillate due to parametric excitation.

References

[1] McDonald, P. H., "Nonlinear Dynamic Coupling in a Beam Vibration," *Journal of Applied Mechanics*, Vol. 22, No. 4, Dec. 1955, pp. 573–578.

[2] Srinivasan, A. V., "Nonlinear Vibrations of Beams and Plates," *International Journal of Nonlinear Mechanics*, Vol. 1, No. 3, Nov. 1966, pp. 179–191.

[3] Eisley, J. G., "Nonlinear Vibrations of Beams and Rectangular Plates," *Zeitschrift fur Angewandte Mathematik und Physik*, Vol. 15, No. 2, March 1964, pp. 167–174.

[4] Eisley, J. G. and Bennett, J. A., "Stability of Large Amplitude Forced Motion of a Simply Supported Beam," *International Journal of Nonlinear Mechanics*, to be published.

[5] Burgreen, D., "Free Vibrations of a Pin Ended Column with Constant Distance Between Ends," *Journal of Applied Mechanics*, Vol. 18, No. 2, June 1951, pp. 135–139.

[6] Lyon, R. H., "Observations on the Role of Nonlinearity in Random Vibrations of Structures," TN D-1872, March 1963, NASA.

[7] Bennett, J. A., "A Multiple Mode Approach to Nonlinear Beam Vibrations," Ph.D. thesis, 1969, Univ. of Michigan, Ann Arbor, Mich.

[8] Grove, W. E., *Brief Numerical Methods*, Prentice-Hall, Englewood Cliffs, N.J., 1966.

[9] Hayashi, C., *Nonlinear Oscillations in Physicsl Systems*, McGraw-Hill, New York, 1964, pp. 89–92.

[10] Pars, L. A., *A Treatise in Analytical Dynamics*, Heineman Educational Books, London, 1965, pp. 461–463.